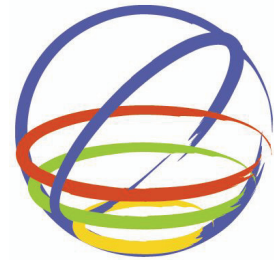


Data Processing and Analysis of Strong Motion Records from the Ms8.0 Wenchuan, China Earthquake

Haiying Yu, Wenxiang Jiang, Yongqiang Yang, Quancai Xie,
Lei Huang, Pingyu Tan, Li Li

Institute of Engineering Mechanics, China Earthquake Administration, Harbin 150080, China



15 WCEE
LISBOA 2012

SUMMARY:

A total of 420 stations of strong motion recordings, (consisting of 1253 individual components), were collected by the China Strong Motion Network Center (CSMNC) after the Wenchuan earthquake. The preliminary processing and analysis of these records is presented in this paper. In order to get the standard format uncorrected accelerograms, the data-format of the original records were transformed. The base-line correction of records was done by CSMNC routinely before the normal processing. There are more than 50 stations with the peak ground acceleration (PGA) larger than 100gal located within the Longmenshan fault zone. Among the 420 stations, 46 are located with a rupture distance of 100km or less. The amount of strong motion records obtained in Chinese Mainland has been significantly increased based on this earthquake, especially the number of near-fault recordings. Based on the collected data, the basic characteristics of the strong ground motions from this earthquake are analyzed. The attenuation relationships of PGAs from the Wenchuan earthquake are given in this article. In addition, shake maps of PGAs are plotted after simulating the PGAs in the near-fault region. The basic characteristics of near-fault ground motion from this event are also summarized, such as the acceleration response spectra, the hanging wall effect, the rupture directivity effect, and the fling step effects. These results can be used as references in the revision of the seismic design code and the reconstruction of disaster area. Finally, the wide application prospect of these records is forecasted.

Supported by: China Earthquake Specialty Science Foundation under Grant No. 201008006; National Natural Science Foundation No. 51178152; CEA,IEM Science Foundation No. 2010C02; National Science and Technology Support Program No. 2009BAK55B01

Keywords: *Wenchuan earthquake, strong motion records, data processing, base-line correction, attenuation relationships*

1. INTRODUCTION

At 14:28 on May 12, 2008, an Ms 8.0 earthquake struck Wenchuan County in Sichuan, China. Its hypocenter was located at 31.021°N latitude and 103.367°E longitude at a depth of 14km. This earthquake took place on the Longmenshan thrust fault. It is the boundary of strong active Qinghai-Tibet Plateau block and inactive Sichuan basin block, cuts off the northwest edge bottom of Sichuan basin, about 400km long, 60km wide. Longmenshan fault is a large-scale compound tectonic zone and composed of 4 large faults, which are Hou-Longmenshan fault (Wenchuan-Maowen fault), central fault (Beichuan-Yingxiuwan fault), Qianshan fault (Guan County-Jiangyou fault) and Shanqian buried fault from west to east respectively. This earthquake occurred on the central fault, which is mainly a thrust fault with a little strike-slip component. Its focal mechanism is complicated^[1]. The unilateral rupture started near the Yingxiu Town of Wenchuan County, extended about 300km to the northeast and passed through Beichuan County. This earthquake was felt throughout China except Heilongjiang, Jilin Province and Xinjiang municipality. The earthquake disasters were extremely serious in Sichuan, Shaanxi and Gansu Province. Between the mainshock occurrence and August 22, 2008, there were a total of 261 aftershocks with $M_s \geq 4.0$, 39 with $M_s \geq 5.0$, 8 with $M_s \geq 6.0$, and the aftershock has a magnitude of 6.4. The distribution of epicenters for the main shock and aftershocks are shown in Figure 1.

There are 420 strong motion stations (including 402 permanent free-field stations, one array for topographical effect and two arrays for structural response observations) which recorded the seismic phase during the earthquake (shown in Figure 2), and most of them obtained the absolute time. Among the 420 stations, more than 50 stations (located in the Longmenshan fault zone and its surrounding areas) had $PGA \geq 100\text{gal}$, and 46 stations are located with rupture distances of less than 100km. The strong motion records from this event are characterized with the digital records, the completed seismic phases and high quality, as well as the detailed site condition of each station. The amount of the near fault strong motion records from Chinese earthquakes has significantly increased and the database of strong motions in China is enriched.

All the stations are equipped with the digital instruments, i.e., GDQJ-II, GDQJ-1A, GSMA-24IP, Etna, K2, GSR-18 and MR-2002 type strong-motion seismographs. Most of these instruments use the SLJ-100 type force-balanced-accelerometer sensors and several Etna-type strong-motion seismographs are equipped with the ES-T type force-balance-accelerometer sensors^[2]. Reference [2] presented a detailed introduction of the China Digital Strong Motion Observation Network and strong motion observation in Wenchuan earthquake.

Shortly after the Wenchuan earthquake, the China Earthquake Administration organized the seismologists from CSMNC, the northwest and southwest sub-center of the China Digital Strong Motion Observation Network (CDSMON) to carry out the mobile observation of strong motions. A mobile array comprised of 59 stations was installed in the seriously affected areas of this event^[3]. To obtain as many records as possible the locations of stations were changed in the area according to the distribution and forecast of aftershocks. Up until the early morning of September 30, 2008 a total of 2,871 recordings of three-component strong motion records observed during the aftershocks were collected by CSMNC.

2. Data-processing of strong motion records

The data-processing of the strong motion records from this earthquake has completed in CSMNC. The conventional process includes: the arrangement, transition, unification of data-format, input and the zero-line correction of the original strong motion records, and then the time-histories of the uncorrected acceleration records are plotted in uniform-format routinely.

The steps of zero-line correction are as follows:

1. Calculate the average acceleration of the first 20 seconds of the original acceleration record;
2. The original acceleration record subtracts the average acceleration;

Followed by the conventional process, the original records are corrected with different bandpass filters separately, and then they are integrated to get the velocities and displacements, the response and Fourier amplitude spectra are also calculated routinely, and finally the time-histories of the uncorrected accelerations, and the corrected accelerations, velocities and displacements, as well as the response and Fourier amplitude spectra of the corrected accelerations are plotted in uniform-format.

3. Statistical analysis of acceleration records

There were a total of 420 stations (belonging to CDSMON) obtained strong motion records in Wenchuan earthquake, and these stations are distributed in 19 provinces (i.e., Sichuan, Yunnan, Gansu, Shaanxi, Ningxia, Qinghai, Shanxi, Shandong, Henan, Hebei, Inner Mongolia, Jiangsu, Fujian, Guangdong, Hubei and Anhui) and municipalities (i.e., Beijing, Tianjin and Shanghai)^[3]. Among the 420 stations, there are 131 ones located in Sichuan province. The time histories of the three-component uncorrected accelerations observed by 21 near-fault stations (Table 1) are plotted in Figure 3. The focal mechanism and finite-fault model for the Wenchuan earthquake released by USGS^[4] are adopted in this article to calculate the rupture distances (the shortest distance between the station

and the fault plane) of 420 stations. The statistical histograms of three-component PGAs from this earthquake are shown in Figure 4. Preliminary analysis of the strong motion records are as follows:

1) There are totally 420 groups of strong-motions events, 7 of them are the case that one of three channels did not get record. Therefore, a total of 1253 components are obtained in this event, and 118 ones with $PGA > 100\text{gal}$.

2) The largest PGA among all records is 957.7gal , which was observed by Wolong station (9.59km to the fault) in Wenchuan County. The second largest one was recorded by Qingping station (0.74km to the fault) in Mianzhu county. The third largest one was got by Bajiao station (13.74km to the fault) in Shifang city. The detailed information of these records such as PGA and dominate frequency (the frequency corresponding to the peak of Fourier amplitude spectrum) is listed in table 2.

3) There are 12 stations with rupture distance (D_{rup}) less than 20km, 11 ones with $20 \leq D_{rup} \leq 50\text{km}$, and 23 stations with $50 \leq D_{rup} \leq 100\text{km}$. Among all the stations got records, the nearest one to the fault is Qingping station about 0.74km to the fault.

4) The PGAs in near-fault region are high, and the largest one approximates to $1g$ (gravitational acceleration). The 90% energy-durations (time intervals between 5-95% of energy) of the records are long, and the average value is about 100sec.

5) The calculated peak ground velocity (PGV) and peak ground displacement (PGD) are high in the near-fault region, and the PGV and PGD of EW component for the Qingping station are as high as 131cm/s and 130cm individually. Figure 5 displays the time-histories of velocity and displacement for the three high amplitude stations: Wolong, Qingping and Bajiao. From the figure, we can see that the PGVs are high and several time histories of velocity are characterized with large velocity pulses.

4. Attenuation relationships of PGAs

Among the 1253 components, there are 419, 420 and 414 ones are in the direction of East-West, South-North and Vertical respectively. Based on the records and the corresponding rupture distances, the attenuation relationships of PGAs can be developed. The ground motion model used in this article is as follows:

$$\log_{10}(PGA) = a + b * \log_{10}(D_{rup} + c)$$

Where PGA denotes the peak ground accelerations in gal; D_{rup} denotes the rupture distance in km; a, b and c are the coefficients to be determined using the method of least-squares and the values of them are listed in Table 3, where σ denotes the regression standard deviation.

The Wenchuan-specific attenuation relationships of PHAs and PVAs described in this section are compared with Huo JR attenuation relationships, which are widely used in Southwest China. The formulas are list in Table 4, where R denotes the rupture distance in kilometers; M is the moment magnitude ^[5]. The PHAs and PVAs regression curves for the Wenchuan earthquake and Huo JR attenuation relationships are shown in figure 6. Huo JR attenuation relationship provides a well estimation of PHAs within 30km of rupture distance and underestimates the PHAs by approximately 10%-30% in medium-far and far distance of 20-200km. And, it provides a better estimation of PVAs within near the fault and overestimates the PVAs by approximately 5%-20% in medium-far and far distance of 10-200km.

5. Shake Maps of PGAs

The destructive power of an earthquake is directly depended on the PGA and the durations of strong motions. The large number of strong motion data recorded in this event can be used to determine the macroscopic epicenter, and they also provide reference for the earthquake disaster evaluation and the

earthquake rescue. Following the method put forward by Chin-Hsiung Loh, the shake maps of PGAs (which is different from the contour maps of the recorded values of PGAs) are plotted in this article. The method is introduced briefly for convenience of understanding. Firstly, we determine the attenuated value for arbitrary site using the attenuation relations of PGA from the Wenchuan earthquake. Then this value is modified according to the recorded values of stations located around the site by means of weighted average. Finally the shake maps of PGA are plotted through interpolation using the natural-neighbor method. It is defined that the estimated PGA values at any stations is expressed as^[6]:

$$\log_{10}(PGA_j) = \log_{10} y(Dist_j, Site_j) + \frac{\sum_{i=1}^n W(D_{ij}) Res_i}{1 + \sum_{i=1}^n W(D_{ij})}$$

Where

$$W(D) = \begin{cases} 1/(D+0.1) & D \leq 20km \\ 0 & D > 20km \end{cases}$$

and $y(Dist, Site)$ denotes PGAs predicted by the attenuation relationships; PGA denotes peak ground acceleration needed to estimate; Dist denotes the distance at site j ; Res_i denotes the residuals for station i (difference between the recorded value and regression value).

Figure 7 displays the shake maps of the three-component PGAs determined using the method mentioned above, and the EW, NS and UD components of PGA are plotted in Figure 7(a), (b) and (c) individually. It is obvious that the distribution of PGA can better represent the hazard distribution of this event. From the figures, we can see that the relative high values of PGA located along the seismogenic fault and confined into a belt zone very close to the fault. In addition, the PGA on hanging wall is larger than that on footwall at the comparable distance, which is caused by the hanging wall/footwall effect on the near-fault ground motions. The PGA in the forward direction of rupture propagation is larger than that in the backward direction, which may be caused by the forward rupture directivity.

6. Response spectra of the uncorrected accelerations

The absolute acceleration response spectra (denoted as response spectra) are computed routinely by CSMNC. The EW, NS and UD components of the 5%-damping response spectra for the 21 near-fault acceleration records are plotted in Figure 8. The dominant periods of response spectra for most records are below 1 sec. The long-period ground motions in the near-fault region are obvious, for some stations, the values of response spectra are still large at natural period of 2s (see Figure 8). However, the long-period ground motions for the records obtained by the stations, Weinan, Xi'an and Xianyang station (Table 5) at the epicentral distance of 691, 637 and 621 km, located far away from the epicenter in the direction of rupture propagation are more obvious. That may be correlated with the local site condition of these stations. The 5%-damping response spectra for Weinan, Xi'an and Xianyang station are plotted in figure 9, which shows that the values of response spectra for the three stations mentioned above are still high at the natural period of 9 sec around. In fact, these three stations are located on the north part of Weinan fault, the middle part of the Weinan downfault basin, and the surround area of the Weinan fault respectively. The site conditions of the three stations are belonged to Class III according to the China Code for Seismic Design of Buildings (GB50011-2001)^[7]. The soft-soil site conditions amplify the ground motions in this region, especially the long-period ground motions. The engineering seismic damages for the Wenchuan earthquake also show that the chimney and high-rising structures are seriously destroyed around the three stations^[8].

7. Conclusions

There was a small amount of strong ground motion accelerograms before the Wenchuan earthquake because of the limited amount of strong-motion stations in Chinese mainland. As for the near-fault records from large earthquakes, the amount is much less. All these things provide an unprecedented opportunity to study the attenuation relationships of strong motion parameters, to revise the seismic ground motion parameter zonation map, and to re-determine the design ground motion parameters. And on this basis, it is much more reasonable and suitable to our national conditions to revise the seismic design code for buildings and structures. This paper just analyzes the effect on condition of sites preliminary, which is worth the further study. Based on the preliminary analysis in this paper, the following conclusions can be drawn:

- 1) The PGAs are large in the near-fault region and the largest PGA among all the acceleration records approximates to 1g. The long duration of strong motion records in this event is another predominant characteristic, and the average value of 90% energy-durations is about 100 sec.
- 2) The calculated peak ground velocity (PGV) and peak ground displacement (PGD) are high in the near-fault region, and both PGV and PGD of the EW component for the Qingping station are as high as 131cm/s and 130cm individually.
- 3) The relative high values of PGA located along the seismogenic fault and confined into a belt zone very close to the fault. The PGA on hanging wall is larger than that on footwall at the comparable rupture distance, and PGA on hanging wall attenuates slower than that on footwall. The PGA in the forward direction of rupture propagation is larger than that in the backward direction.
- 4) The long-period ground motions in the near-fault zone are obvious; however, those of stations (such as Weinan, Xi'an and Xianyang station) located far away from epicenter in the forward direction of rupture propagation are more obvious, which may be caused by the local site condition and geological environment in this region.
- 5) The large number of records obtained in this event greatly enlarges the database of strong motions in China, and fill the domestic gap in the near-fault strong ground motions at the same time.

Data and Resources

Data used in this study can be obtained from the China Strong Motion Network Center at www.csmnc.net.

Acknowledgements

The authors are very grateful to CSMNC for providing strong motion data. Especially are grateful to the substantial support from the Department of Seismic Disaster Prevention, China Earthquake Administration. We also wish to express our deepest gratitude to Prof. Zhou Yongnian and Li Xiaojun for their valuable suggestions. Thanks to the strong motion observed personnel from the Seismological Bureau of Sichuan, Yunnan, Gansu, Shaanxi, Ningxia, Qinghai, Shanxi, Shandong, Henan, Hebei, Beijing, Tianjin, Inner Mongolia, Jiangsu, Shanghai, Fujian, Guangdong, Hubei and Anhui provinces/municipalities and those from Institute of Engineering Mechanics, China Earthquake Administration for their hard works of strong motion observation and the collecting of records.

References

1. Chen, Yuntai, Xu, Lisheng, et al. (2008). Analysis of the Source Characteristics of the Wenchuan Earthquake of May 12, 2008, Report by the Institute of Geophysics (<http://www.cea-igp.ac.cn>), China Earthquake Administration on the Wenchuan Earthquake, 2008. (in Chinese)
2. The Department of Seismic Disaster Prevention, China Earthquake Administration, The

uncorrected acceleration for Ms8.0 Wenchuan Earthquake, The report for China strong motion records, Vol.12, No.1, Earthquake Publishing Press, 2008. (in Chinese)

3. Li XJ, Zhou ZH, Yu HY, Wen RZ, Lu DW, Huang M, Zhou YN and Cui JW, 2008. Strong motion observation and recordings from the great Wenchuan earthquake. [J]. *Earthquake Engineering and Engineering Vibration* 3, 235-246,
4. Chen Ji and Gavin Hayes 2008. 'Finite fault model-Preliminary result of the May 12, 2008 Mw 7.9 Eastern Sichuan, China earthquake' report by U.S. Geological Survey. (<http://earthquake.usgs.gov/eqcenter/eqinthenews/2008/us2008ryan/finitefault.php>, last accessed Nov 16th, 2008)
5. Huo Junrong, 1989. Study on the attenuation laws of strong earthquake ground motion near the source. PhD Dissertation. Institute of Engineering Mechanics, China Earthquake Administration. (In Chinese)
6. Chin-Hsiung Loh, Zheng-kuan Lee, Tsu-Chiu Wu and Shu-Yuan Peng, 2000, Ground motion characteristics of Chi-Chi earthquake of 21 September 1999. *Earthquake Engng & Struct. Dyn.* 29:867-897.
7. China Ministry of Construction, 2001, "Code for Seismic Design of Buildings" (GB 50011-2001), China Construction Industry Printing House, Beijing. (In Chinese)
8. Sun Jingjiang, Tang Yuhong, Sun Zhongxian, Zheng Chao, Shi Hongbin, Lin Lin, 2009. Damage to urban buildings in zones with intensity VIII or VII during Wenchuan earthquake and discussions on some typical damage. *Journal of Earthquake Engineering and Engineering Vibration.* 29(6): 65-73. (In Chinese)

Table 1. Station parameters and PGAs of the 21 stations near to the fault

| Station | Code | Long. (E) | Lat. (N) | Elevation (m) | D _{rup} (km) | PGA (gal) | | |
|--------------|-------|-----------|----------|------------------|--------------------------|-----------|----------|----------|
| | | | | | | EW | NS | UD |
| Tashui | 51AXT | 104.30 | 31.54 | 548.0 | 26.10 | -289.540 | 203.450 | 179.926 |
| Minzhi | 51BXZ | 102.88 | 30.49 | 1200.0 | 25.40 | 153.251 | -117.085 | 109.241 |
| Shijing | 51GYS | 105.84 | 32.15 | 889.0 | 53.63 | 320.485 | 273.971 | -143.700 |
| Zengjia | 51GYZ | 106.10 | 32.62 | 1350.0 | 60.09 | 424.480 | -410.481 | -183.338 |
| Shuangliusuo | 51HSL | 103.26 | 32.06 | 2015.0 | 64.40 | -107.640 | -142.561 | -108.970 |
| Chonghua | 51JYC | 104.99 | 31.90 | 588.0 | 18.49 | 297.187 | 278.961 | -180.489 |
| Jiangyou | 51JYD | 104.74 | 31.78 | 530.0 | 18.76 | -511.330 | 458.680 | -198.278 |
| Hanzeng | 51JYH | 104.63 | 31.78 | 575.0 | 11.11 | -519.491 | -350.135 | -444.331 |
| Guoyuan | 51JZG | 104.32 | 33.12 | 1825.0 | 85.58 | -169.741 | 241.450 | 109.258 |
| Muka | 51LXM | 103.34 | 31.57 | 1490.0 | 14.28 | 320.938 | -283.840 | 357.810 |
| Shaba | 51LXS | 102.91 | 31.53 | 1491.0 | 41.52 | 221.260 | 261.755 | 211.088 |
| Taoping | 51LXT | 103.45 | 31.56 | 1487.0 | 10.79 | 339.733 | 342.381 | 379.577 |
| Diexi | 51MXD | 103.68 | 32.04 | 2328.0 | 36.56 | 246.493 | -206.210 | -143.910 |
| Nanxin | 51MXN | 103.73 | 31.58 | 1610.0 | 15.66 | -421.281 | 349.239 | -352.480 |

| | | | | | | | | |
|----------|-------|--------|-------|--------|-------|----------|----------|----------|
| Maoxian | 51MXT | 103.85 | 31.68 | 1575.0 | 16.18 | -306.571 | 302.163 | -266.640 |
| Qingping | 51MZQ | 104.09 | 31.52 | 920.0 | 0.74 | -824.121 | 802.710 | 622.910 |
| Muzuo | 51PWM | 104.52 | 32.62 | 1829.0 | 31.64 | 273.744 | 287.370 | 177.370 |
| Bajiao | 51SFB | 103.99 | 31.28 | 765.0 | 13.74 | 556.169 | -581.592 | 633.090 |
| Wolong | 51WCW | 103.18 | 31.04 | 919.0 | 9.59 | 957.700 | 652.851 | 948.103 |
| Wenxian | 62WIX | 104.48 | 32.95 | 980.0 | 62.64 | -142.691 | -141.157 | -131.973 |
| Wudu | 62WUD | 104.99 | 33.35 | 955.0 | 69.35 | -184.874 | -163.990 | 108.611 |

Table 2. The three-component PGAs and dominant frequencies for three typical records in Wenchuan earthquake

| Station Name | EW | | NS | | UD | |
|--------------|----------|------------------------|----------|------------------------|----------|------------------------|
| | PGA(gal) | Dominant frequency(Hz) | PGA(gal) | Dominant frequency(Hz) | PGA(gal) | Dominant frequency(Hz) |
| Wolong | 957.7 | 2.4 | 652.9 | 5.5 | 948.1 | 8.1 |
| Qingping | -824.1 | 1.9 | 802.7 | 1.5 | 622.9 | 11.0 |
| Bajiao | 556.2 | 3.4 | -581.6 | 3.4 | 633.1 | 7.6 |

Table 3. The regress coefficients for PGAs from the Wenchuan earthquake

| Component | a | b | c | σ |
|------------|-------|--------|--------|----------|
| Horizontal | 5.308 | -1.485 | 42.067 | 0.324 |
| Vertical | 4.275 | -1.293 | 13.402 | 0.258 |

Table 4. Attenuation formulas and standard deviations of Huo JR(1989) attenuation relationships

| Attenuation formulas | σ |
|--|----------|
| $\lg a_{pH} = 0.163 + 0.722M - 1.842 \lg(R + 0.125e^{0.727\lambda})$ | 0.339 |
| $\lg a_{pV} = -0.148 + 0.794M - 2.114 \lg(R + 0.125e^{0.72})$ | 0.358 |

Table 5. Station parameters and PGAs of Weinan, Xian and Xianyang station

| Station | Code | Long. (E) | Lat. (N) | Elevation (m) | D _{epi} (km) | PGA (gal) | | |
|----------|-------|-----------|----------|---------------|-----------------------|-----------|--------|---------|
| | | | | | | EW | NS | UD |
| Weinan | 61WEN | 109.49 | 34.53 | 317.0 | 691.0 | -35.908 | 30.595 | -14.022 |
| Xian | 61XIA | 108.95 | 34.21 | 432.0 | 637.0 | 52.714 | 44.587 | -13.351 |
| Xianyang | 61XYT | 108.70 | 34.35 | 412.0 | 621.0 | 40.103 | 33.289 | 18.063 |

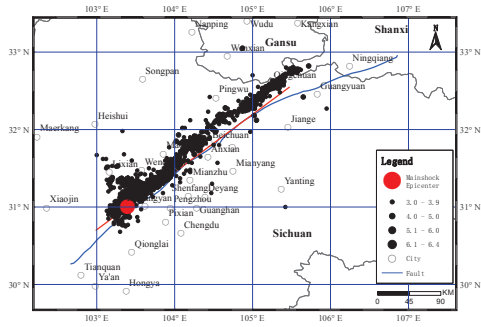


Figure 1. Locations of the epicenters for the main shock and aftershocks of the Wenchuan earthquake

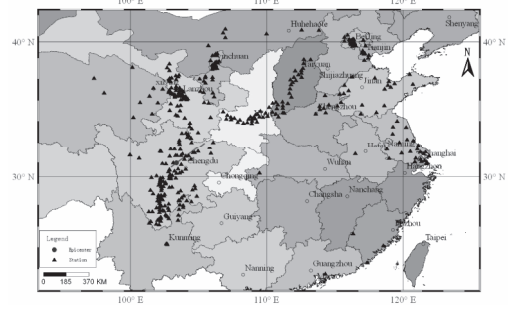


Figure 2 Locations of 420 stations obtained records in the Wenchuan earthquake

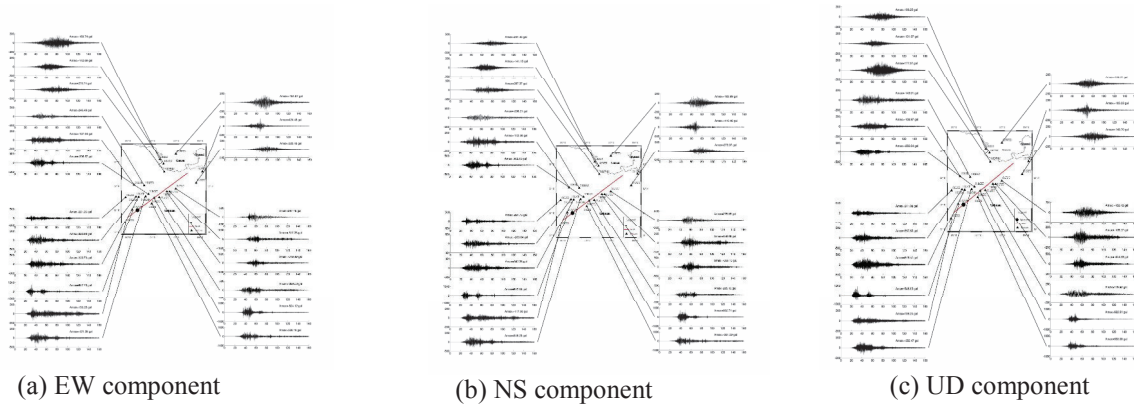


Figure3 The time-histories of the three-component uncorrected accelerations for 21 near-fault stations from the Ms 8.0 Wenchuan earthquake

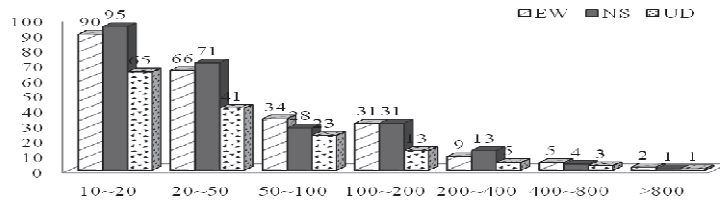
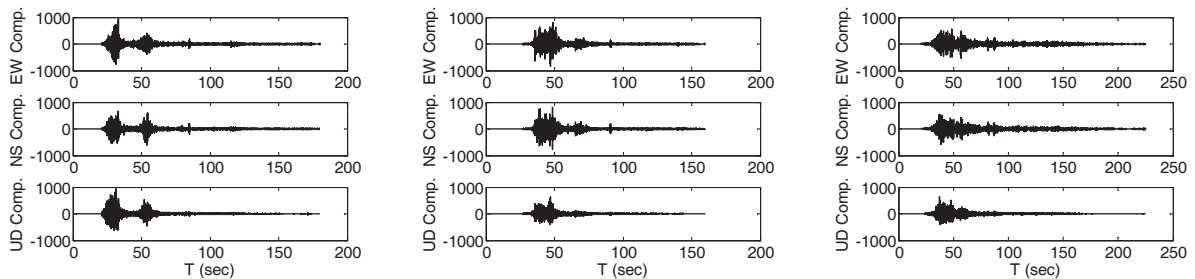
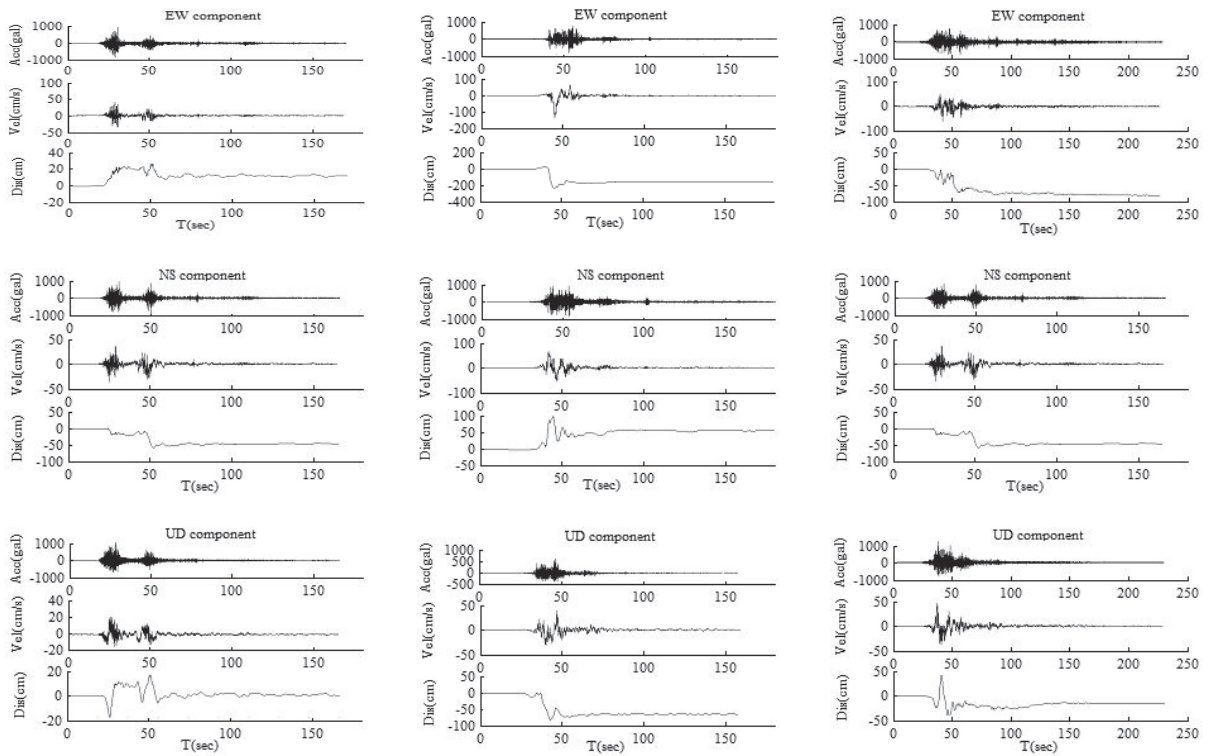


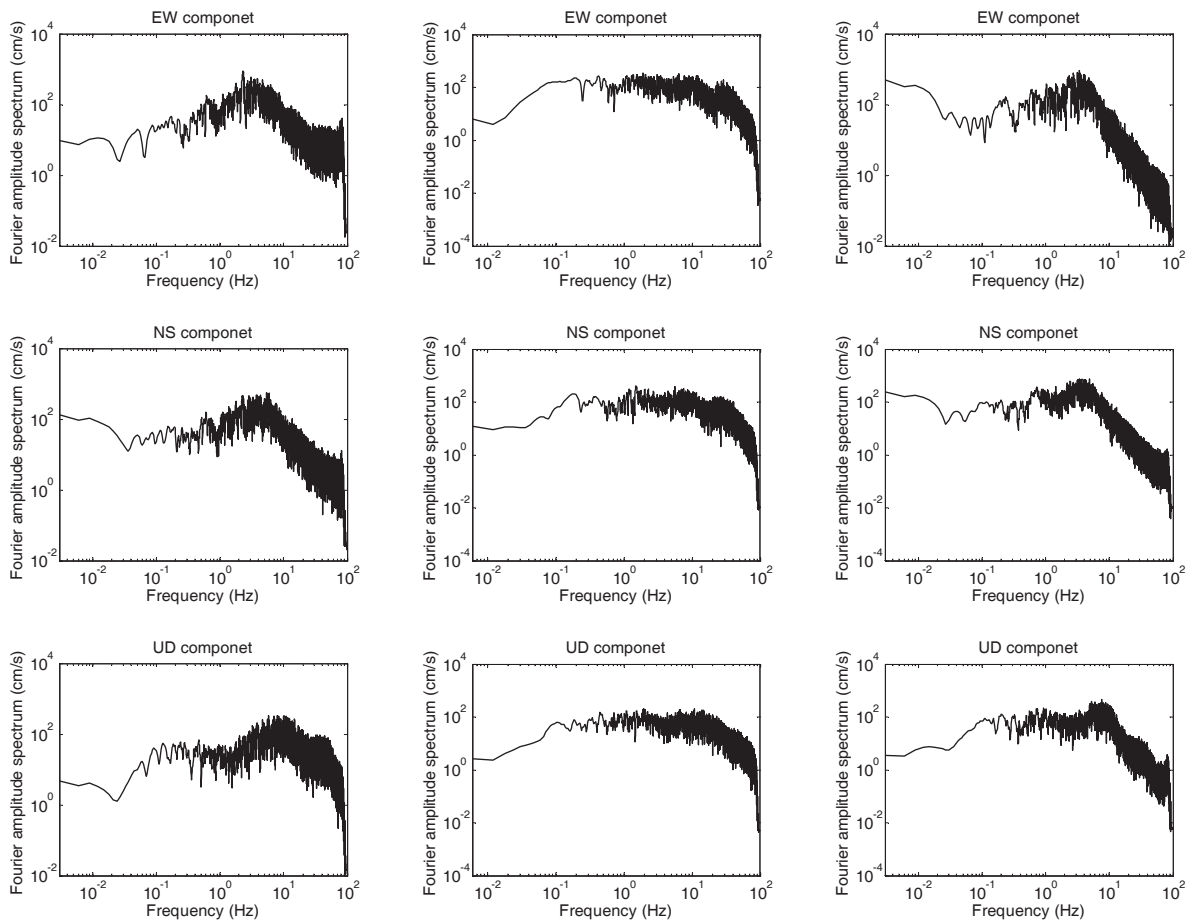
Figure 4 The statistical histogram for the three-component PGAs from the Wenchuan earthquake



(a) The time-histories of the uncorrected accelerations



(b) The time-histories of the three-component corrected accelerations, velocities and displacements



(c) Fourier amplitude spectra of the uncorrected accelerations

Figure 5. The time-histories of (a) the uncorrected accelerations, (b) the corrected accelerations, velocities and displacements, (c) Fourier amplitude spectrum of the uncorrected acceleration for three typical stations: Wolong (left), Qingping(middle) and Bajiao(right) station

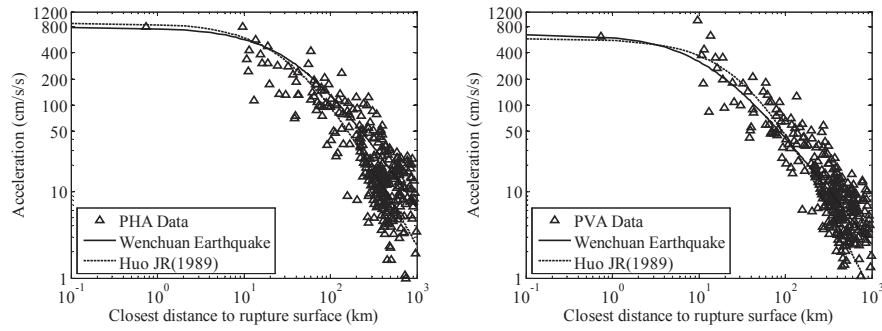


Figure 6. The Wenchuan earthquake specific regress curves of PGA for horizontal component (left) and vertical component(right)

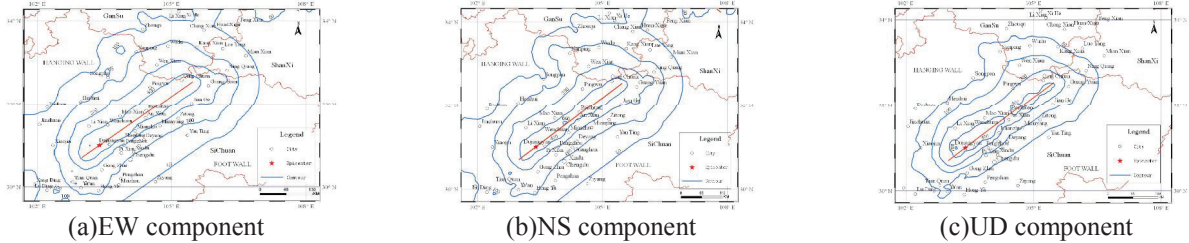


Figure 7 The shake maps of three-component PGA from the Ms 8.0 Wenchuan earthquake

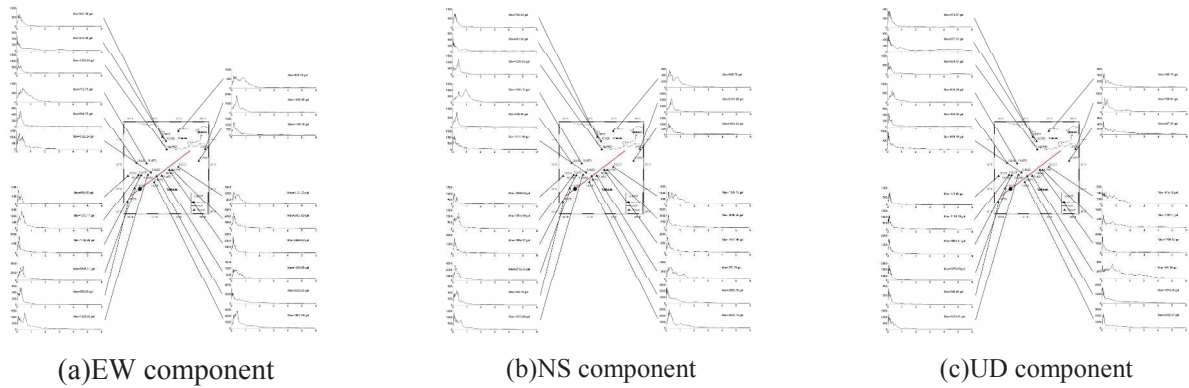


Figure 8. The 5%-damping absolute acceleration response spectra (damping ratio of 5%) for the (a) EW, (b) NS and (c)UD component of uncorrected accelerations recorded by 21 near-fault stations

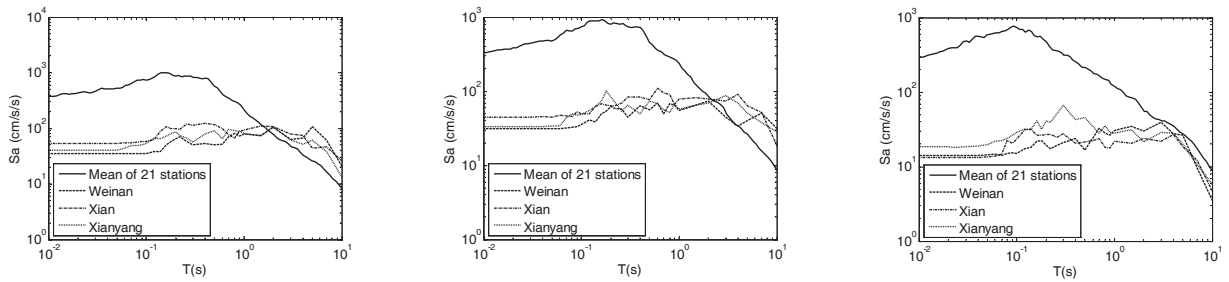


Figure 9 Absolute acceleration response spectra for EW, (Upper left), NS (Upper right) and UD component (Bottom) of the uncorrected accelerations recorded by Weinan, Xi'an and Xianyang stations